https://doi.org/10.5194/egusphere-2024-641
Preprint. Discussion started: 14 March 2024

Interannual Variations of Terrestrial Water Storage in the East African Rift Region

Eva Boergens[1], Andreas Güntner[1,2], Mike Sips[1], Christian Schwatke[3], and Henryk Dobslaw[1]

[1]GFZ German Research Centre for Geosciences, Telegrafenberg, 14473 Potsdam, Germany
[2]University of Potsdam, Institute of Environmental Sciences and Geography, 14469 Potsdam, Germany
[3]Technical University of Munich, School of Engineering & Design, Department of Aerospace & Geodesy, Deutsches Geodätisches Forschungsinstitut (DGFI-TUM), Arcisstraße 21, 80333 München, Germany

Correspondence: Eva Boergens (boergens@gfz-potsdam.de)

Abstract. The US-German GRACE (Gravity Recovery and Climate Experiment, 2002-2017) and GRACE-FO (GRACE-Follow-On, since 2018) satellite missions observe terrestrial water storage (TWS) variations. Over twenty years of data allow for investigating interannual variations beyond linear trends and seasonal signals. However, the origin of observed TWS changes, whether naturally caused or anthropogenic, cannot be determined solely with GRACE and GRACE-FO observations. This study focuses on the East African Rift region region around lakes Turkana, Victoria, and Tanganyika. It aims to characterise and analyse the interannual TWS variations together with surface water and meteorological observations and determine whether natural variability or human interventions caused these changes.

To this end, we apply the STL method (Seasonal Trend decomposition based on Loess) to separate the TWS signals into a seasonal signal, an interannual trend signal, and residuals. By clustering these interannual TWS dynamics for the African continent, we define the exact outline of the study's region.

In this area, a TWS decrease until 2006 was followed by a steady increase until around 2016, and Africa's most significant TWS increase occurred in 2019 and 2020. We found that besides precipitation and evaporation variability, surface water storage variations in the large lakes of the region explain large parts of the TWS variability. Storage dynamics of Lake Victoria regulated by the Nalubaale Dam alone contribute up to 50% of the TWS changes. Satellite altimetry reveals the anthropogenically altered discharge downstream of the dam. It thus indicates that human intervention in the form of dam management at Lake Victoria substantially contributes to the TWS variability seen in the East African Rift region.

1 Introduction

Satellite gravimetry, as realised with the Gravity Recovery And Climate Experiment (GRACE, 2002-2017) satellite mission and its successor GRACE-Follow-On (GRACE-FO, since 2018) is the only remote sensing technique available today that provides quantitative estimates of water storage changes on regional to global scales. These observations cover equally surface

https://doi.org/10.5194/egusphere-2024-641
Preprint. Discussion started: 14 March 2024

and subsurface water storage compartments, i.e., they represent changes in the complete water column, including all types of surface water bodies, soil moisture, snow, ice, and groundwater. That makes the GRACE and GRACE-FO data a unique and invaluable complement to all other existing observations of the hydrological cycle.

Both GRACE and GRACE-FO satellite missions measure tiny variations in the distance between two twin satellites trailing each other in a polar orbit at very low (500 km) altitudes (Tapley et al., 2004; Landerer et al., 2020). From collecting these variations along the satellite orbits, the current gravity field of the Earth can be derived. By computing and comparing monthly global gravity fields, gravity's spatial and temporal variations and, thus, the underlying mass variations on and below the Earth's surface can be investigated. The applications of GRACE/GRACE-FO data in hydrology are manifold and include, for instance, assessing water balance closure at regional to global scales (Lehmann et al., 2022), quantifying the ice mass loss of the continental ice-sheets (Sasgen et al., 2020), groundwater storage changes (Frappart and Ramillien, 2018), water storage capacity and flood potential (Reager and Famiglietti, 2009) or drought effects e. g. in Central Europe (Boergens et al., 2020b). Tapley et al. (2019) gives a comprehensive summary of state-of-the-art applications of GRACE data for climate and hydrological research.

Quantifying large-scale terrestrial water storage (TWS) variations on the continents has been one of the primary fields of application of GRACE data. Several publications investigated TWS variations in Africa at regional to continental scales. For example, Frappart (2020) analysed the groundwater storage in the Sahara aquifer systems with GRACE data, while Ferreira et al. (2018) combined TWS and surface water storage in the Niger Basin in West Africa. Scanlon et al. (2022) investigated hydrological extremes in Africa by considering climatic teleconnections. Of all continents, only Africa had an overall positive linear TWS trend of about $2\,\mathrm{mm/year}$ (corresponding to $62\,\mathrm{Gt/year}$) over the last 21 years (Figure 1a). Thus, the continent has been gaining water over the last two decades, although the observed amplitude of the signal is smaller than for most other continents. The spatial trend patterns, though, are heterogeneous (Figure 1b). Two regions stand out with positive TWS trends for the GRACE/GRACE-FO period: the Niger basin and the East African Rift region. The area surrounding Lake Victoria exhibits the most distinct trend of the region. This study focuses on the East African Rift region around Lake Victoria.

The East African Rift region is characterised by large lakes, including Lake Victoria, the second largest freshwater lake in the world (by area), Lake Tanganyika, and Lake Turkana. The region's lakes have been named one of the Global 200 eco-regions for conservation by the World Wide Fund for Nature (WWF), emphasising their importance for hydrology and ecosystems (Olson and Dinerstein, 2002).

The climate of the East African Rift region is tropical, with a semiannual precipitation signal. The primary rainy season is from March to May, and the secondary rainy season is from October to December (Yang et al., 2015). However, substantial interannual variability in precipitation and evaporation have been observed in the past (Ummenhofer et al., 2018). To investigate long-term interannual variations in precipitation and evaporation, especially in the context of drought monitoring, standardised indices got well established, namely the Standardised Precipitation Index (SPI) (McKee et al., 1993) and Standardised Precipitation Evaporation Index (SPEI) (Vicente Serrano, S.M., Beguiria, S. & Lopez-Moreno, 2010). Both indices have been applied in regional studies in East Africa. For example, Ayugi et al. (2020) employed the SPEI to investigate droughts and floods in Kenya, or Uwimbabazi et al. (2022) used both SPI and SPEI for their investigation of changes in droughts over Rwanda.

https://doi.org/10.5194/egusphere-2024-641
Preprint. Discussion started: 14 March 2024

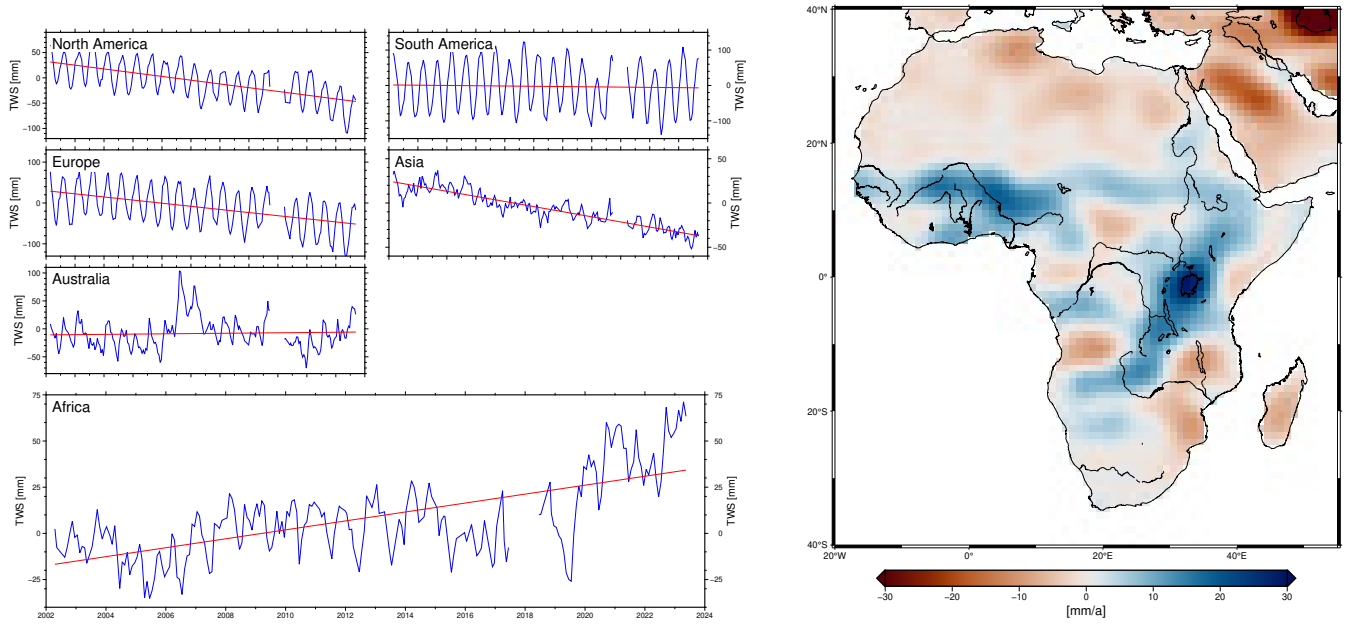

(a) Monthly area-average TWS variations and long-term trends for all continents

(b) TWS trends for the period 2002 to 2023 in Africa

Figure 1. Terrestrial water storage (TWS) trends from GRACE/GRACE-FO satellite gravimetry (COST-G/GravIS data set, see subsection 2.1)

Surface water storage variations are by now commonly monitored by satellite altimetry. Altimetry measures the water level variations of lakes, rivers, or wetlands (e. g. Schwatke et al., 2015) while surface water body extent can be monitored by remote sensing satellites (e. g. Pekel et al., 2016; Schwatke et al., 2019). With these two observations, storage variations are estimated. Tong et al. (2016) combined altimetric water levels and surface area extent to investigate surface water storage variations in East Africa, while Herrnegger et al. (2021) employed water level data of smaller lakes in Kenya to investigate the hydroclimatic conditions of the region. The large lakes of the East African rift have been the subject of earlier research with multiple sensors and a particular focus on Lake Victoria (e. g. Swenson and Wahr, 2009; Velpuri et al., 2012; Hassan and Jin, 2014).

Earlier studies on TWS changes in the East African Rift region include Becker et al. (2010), who used GRACE data together with altimetric water level observations and found both an influence of the Indian Ocean Dipole and surface water storage on TWS. The former result was confirmed by Anyah et al. (2018), who investigated connections between climate indices and TWS and found a strong influence of the Indian Ocean Dipole on TWS in the East African Rift region, too. However, at the same time, part of the region is among the most densely populated areas in Africa (Salvatore et al., 2005), which influences the hydrology through human interventions such as the construction of large dams along the major rivers (Getirana et al., 2020). Most notably, Lake Victoria, which exhibited strong fluctuations in its water levels in the last decades, has been dammed since the 1950s by the Nalubaale dam (formerly known as Owens-Falls dam), which raised the water level of the lake by about 2 m (Okungu et al., 2005). In the years between 2003 and 2006, the region exhibited a drought which naturally lowered the

https://doi.org/10.5194/egusphere-2024-641
Preprint. Discussion started: 14 March 2024

water levels of Lake Victoria, while at the same time, the water extraction at the dam was increased, which further declined the water levels (Sutcliffe and Petersen, 2007; Kull, 2006; Awange et al., 2008). Intense rainfall events in 2019/2022 led to a rapid rise of water levels, causing massive floodings along the shores (Khaki and Awange, 2021). Several recent studies found with hydrological modelling, that a large part of the observed storage variation of Lake Victoria is due to human intervention and not naturally occurring (Vanderkelen et al., 2018; Getirana et al., 2020). In contrast, in their study on TWS trends at the global scale, Rodell et al. (2018) labelled the trend in TWS around Lake Victoria as "probable natural variability".

In this study, we investigate the long-term interannual TWS variations in the East African Rift region (section 3). The link between these interannual variations and both meteorological data (section 5) and surface storage variations (section 6) will be investigated. We strive to give additional evidence of whether the observed storage trends are of climatic or anthropogenic origin (section 7).

2 Data

2.1 GRACE/GRACE-FO TWS Data

This study uses 221 monthly GRACE and GRACE-FO gravity fields from the COST-G RL01 (GRACE) and RL02 (GRACE-FO) data set (Jäggi et al., 2020; Meyer et al., 2023). The data set is the result of the IAG (International Association of Geodesy) Services "International Combination Service for Time-variable Gravity Fields (COST-G)" in which seven different solutions of GRACE data processing centres are combined at the University of Bern. From these monthly gravity fields global 1° TWS are derived (Boergens et al., 2020a) which are freely and publicly available from the GravIS portal (gravis.gfz-potsdam.de, TWS V.0005). Details of the processing steps can be found in Dobslaw and Boergens (2023).

2.2 Precipitation Data and Precipitation Indices

We analyses both precipitation data and subsequently derived standardised meteorological indices in this study. We use the monthly Global Precipitation Climatology Centre (GPCC) precipitation data set, given globally on a 1°grid until the end of 2019 (Schneider et al., 2022). After January 2020, the First Guess GPCC monthly data is used, given in the same spatial resolution (Ziese et al., 2011). As the latter data set contains data since 2004, we verify the consistency between the two in the overlapping period. Besides monthly precipitation, we consider accumulated precipitation time series. To this end, the value of each month is the accumulated precipitation over the preceding n months.

Furthermore, we use the "Standardised Precipitation Evaporation Index" (SPEI) (Vicente Serrano, S.M., Beguiria, S. & Lopez-Moreno, 2010). SPEI is based on a combination of precipitation with (potential) evaporation. For the index, the precipitation minus evaporation values $P - E$ accumulated over a fixed period n such as six, twelve, 24, or 48 months $\overline{P - E}_n$ are compared to the distribution of this quantity in the same month over the whole time series. From this statistical distribution, which is not necessarily normal, the mean value μ_j and the standard deviation σ_j for a given month j are calculated. The index

https://doi.org/10.5194/egusphere-2024-641
Preprint. Discussion started: 14 March 2024

$SPEI(t,j)$ is then computed with

$$SPEI(t,j) = \frac{\overline{P-E}_n(t,j) - \mu_j}{\sigma_j}. \quad (1)$$

Values of SPEI between -1 and 1 indicate near normal conditions, while with values below -1, the conditions are drier and above 1, wetter than usual.

We rely on pre-computed SPEI data sets. The Instituto Pirenaico de Ecología, Zaragoza, Spain (https://spei.csic.es/database.html) provides two different SPEI realisations. The first, the SPEI Global Drought Monitor, is based on the GPCC first look precipitation data set and uses the NOAA NCEP CPC_GHCN CAMS gridded dataset for mean temperature (Fan and van den Dool, 2008) from which the potential evaporation is computed via the Thornthwaite equation. This SPEI is recommended for near-real-time applications. The second, the Global SPEI database (SPEIbase, v2.9), uses the CRU TS 4.03 precipitation data and the FAO-56 Penman-Monteith estimation for potential evaporation (Vicente Serrano, S.M., Beguiria, S. & Lopez-Moreno, 2010; Beguería et al., 2010, 2014). This SPEI offers more long-term, robust information. We employed both SPEI variants (called SPEI (GPCC-based) and SPEI (CRU-based) in the following) to assess the influence that different precipitation data sets might have.

2.3 Lake Data

We now analyse the water volume changes of the major lakes of the East African Rift Region. Figure 2 gives an overview of the region. Among the lakes, there are some of the world's largest freshwater bodies. Lake Victoria is the second largest (by area, ninth by volume), and Lake Tanganyika is the sixth largest (by area, second by volume) freshwater lake.

We derive the water volume change of the lakes from altimetric water level and lake surface extent data. The water level time series are based on multi-mission satellite altimetry, freely available on the "Database for Hydrological Time Series of Inland Waters" (DAHITI, https://dahiti.dgfi.tum.de) web portal maintained by the "Deutsches Geodätisches Forschungsinstitut der Technischen Universität München" (DGFI-TUM).

The DAHITI approach for estimating water level time series is based on a Kalman filtering approach and an extended outlier rejection, described in detail in Schwatke et al. (2015). All applied geophysical corrections and models are identical for all altimeter missions, including a multi-mission cross-over analysis to derive homogeneous water level time series from various satellites. The time series length varies and falls between September 1992 and September 2023, depending on the crossing altimeter tracks. The temporal resolution depends on the number of altimeter crossings and the repeat cycle of the used altimeter mission and can vary between a few days and about a month.

To assess the area of the lakes in the East African Rift Region, we analysed the Global Surface Water Occurrence maps provided by Pekel et al. (2016) via the Global Surface Water Explorer (https://global-surface-water.appspot.com/). The data set is based on 36 years (1984-2020) of global remote sensing observations of water surfaces, classified to a water occurrence probability for each pixel. I. e. permanent water bodies have a water occurrence probability of 100%, while lake shores have a probability below 100% but above 0% due to varying water levels. However, as a result of cloud cover or similar effects in the remote sensing data, some pixels, even in the middle of permanent lakes, do not reach 100% water occurrence. Thus, we

https://doi.org/10.5194/egusphere-2024-641
Preprint. Discussion started: 14 March 2024

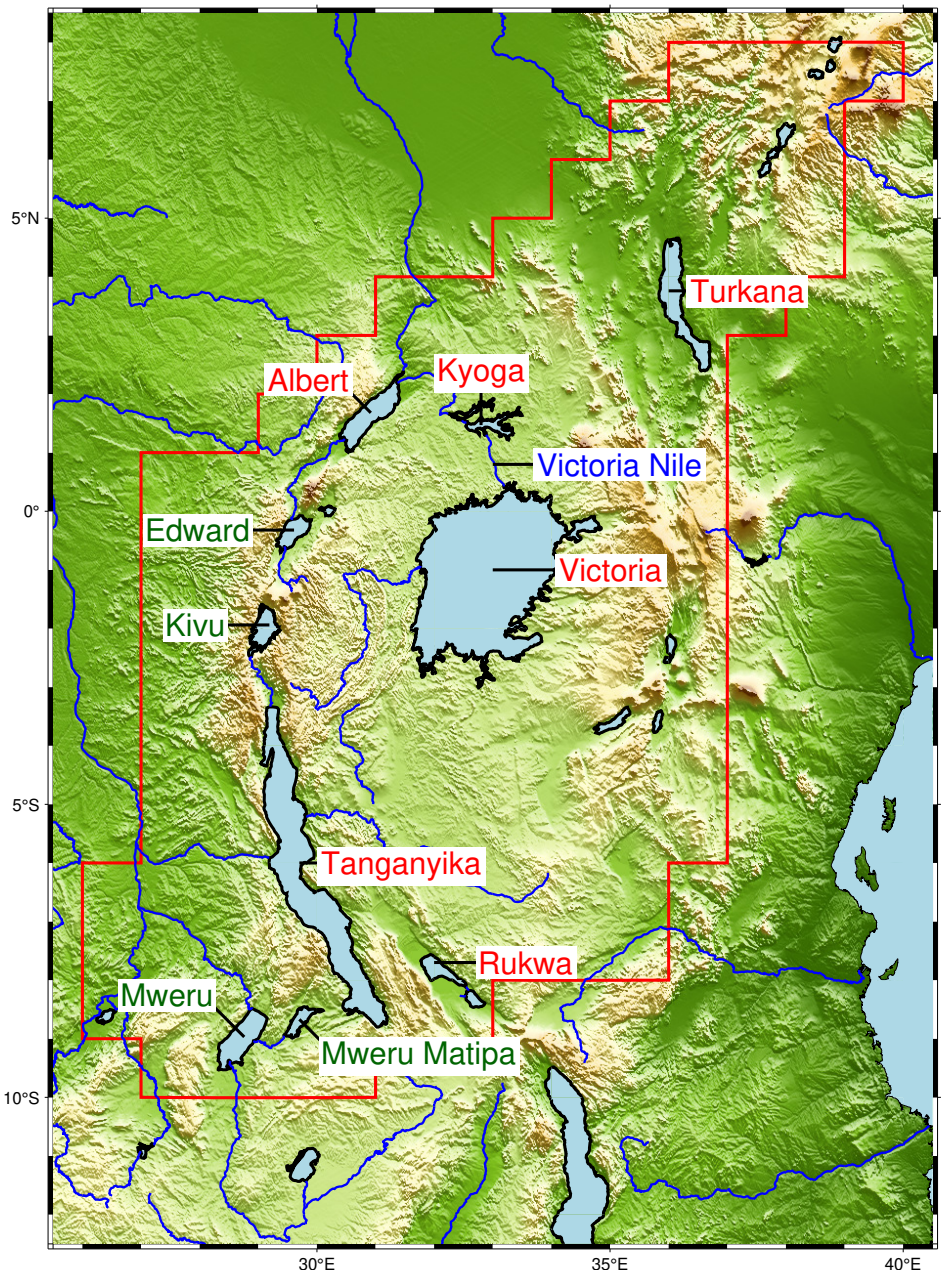

Figure 2. East African Rift Region: Study area and major lakes. The red outline delineates the study area considered here. For lakes labelled in red, we analyse water storage changes individually; lakes labelled in green are summarised later as small lakes (see Figure 12).

https://doi.org/10.5194/egusphere-2024-641
Preprint. Discussion started: 14 March 2024

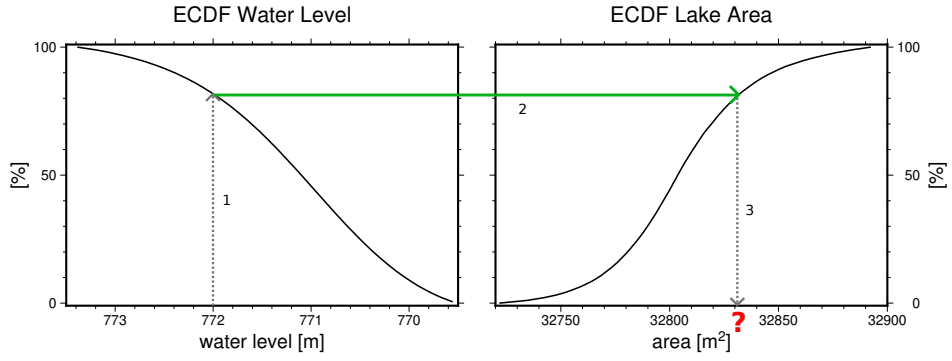

Figure 3. Example of the water level and surface area empirical cumulative distribution function (ECDF) for Lake Tanganyika. Procedure to get surface area from a given water level: Step 1 - for water level read quantile of ECDF; Step 2 - look up same quantile in lake area ECDF; Step 3 - get lake area to this quantile.

considered all occurrence probabilities larger than 95% as permanent water. From these water occurrence maps we estimate an empirical cululative distribution function (ECDF) of lake surface area.

Similar to the ECDF of the lake surface area, we also derived the ECDF of water levels from the level time series of each lake. Assuming a monotone and continues relationship between lake height and lake area, the two ECDFs can be used to map the lake area for each water level observation. Figure 3 illustrates the procedure on the example of Lake Tanganyika. For a given water level, its lake level ECDF quantile is read (step one), i.e. the percentage of observed water levels equal or lesser. The same quantile is looked up in the lake area ECDF (step 2) and, thus, the corresponding lake area can be determined (step 3). With this procedure we get for every water level value an associated lake area.

Thus, from the time series of water level (H) and of lake area (A), the water volume change ΔV_i between the time steps t_{i-1} and t_i was calculated with a truncated pyramid formula:

$$\Delta V_i = \frac{1}{3}\left(H_i - H_{i-1}\right)\left(A_i + A_{i-1} + \sqrt{A_i A_{i-1}}\right). \tag{2}$$

Finally, to get the time series of lake volume V relative to the first time step, all ΔV_i are cumulated.

In order to compare the spatial distribution of the lake storage to TWS observed by satellite gravimetry, it needs to be filtered to get a comparable spatial resolution to the TWS data. To this end, we first interpolate each volume time series to monthly values and distribute the volume uniformly over the lake's surface to get equivalent water heights. Then, we employ a Gaussian filter with a half-width of 350 km, to mimic the spatial resolution of TWS. Such filtered surface water storage (SWS) maps can be compared to TWS maps.

3 Time Series Analysis

A simple time series decomposition into periodic seasonal annual and semiannual signals and linear trend is not well suited to characterise the temporal variations of TWS in Africa over the available 21 years due to substantial interannual variability.

https://doi.org/10.5194/egusphere-2024-641
Preprint. Discussion started: 14 March 2024

Thus, we employed the Seasonal-Trend Decomposition with Loess (STL) method to separate the TWS signals into an annual, trend, and residual signal (Cleveland et al., 1990). The so-called trend component of the STL decomposition contains not only a linear trend but all multi-year interannual variations. The second advantage of STL compared to a conventional parametric decomposition is its ability to capture changing seasonal amplitudes over the time series.

The results of the STL decomposition depend on several parameters that govern the smoothness of the trend and the annual signal. Cleveland et al. (1990) provided guidelines for choosing the STL parameters, which we used with empirical testing and visual inspection, resulting in the following parameter values. n_p: Length of annual signal, 12 in our case; n_i and n_o: the number of passes through the inner and outer loop, respectively, set to 1 and 10; n_l: the width of the low-pass filter, set to 13; and n_t and n_s: the trend and seasonal signal smoothing parameter, both set to 35.

Problems for STL in sorting out the interannual signal component arise around the data gap between the GRACE and GRACE-FO satellite missions in 2017/2018. The standard STL approach linearly interpolates across data gaps, which is inappropriate here due to seasonality. Figure 4 displays the data gap problem based on a hypothetical data-gap (Dec. 2006 to Feb. 2008) in the GRACE-only time series. In blue, the resulting separated signals of the original signal are displayed, and red shows the results in the presence of a data gap. While the annual signal is barely affected, the interannual trend signal exhibits unexpected behaviour before and after the data gap.

To overcome this problem, we implemented a more sophisticated gap-filling approach. We took the STL described above in the first step to identify the annual signal. This annual signal was then removed from the original time series. The data gaps are linearly interpolated in the resulting residual time series, and then the annual signal is added back. This gap-filled time series (i.e., filled with an annual signal plus linear trend) was, in turn, used as input to the STL decomposition. Finally, the periods of the data gaps were masked out again for further analysis and presentation. Returning to the example time series separation above, Figure 4 shows in green the resulting separated signals after we filled the hypothetical gap in 2007. The interannual trend is significantly closer to the interannual trend without data gap and the unexpected peaks before and after the data gap have vanished.

We applied the STL decomposition with gap filling to the TWS time series of all grid cells of Africa. As we seek to investigate the interannual TWS behaviour in this study, we will base all subsequent analyses only on the STL interannual trend component.

4 Clustering of Interannual TWS Variations

The visual inspection of the TWS interannual trend components revealed similar temporal patterns in regions that were often incongruent with river basins or climate zones. Thus, we employed a cluster analysis to identify regions of similar temporal TWS dynamics.

A cluster analysis aims at grouping data items into subsets such that the elements within each cluster have a high degree of similarity among themselves and are relatively distinct from elements assigned to other clusters (see, e.g. Hastie et al. (2009) for an overview of cluster analysis algorithms). We applied an hierarchical approach (Ward, 1963) for which no assumptions

https://doi.org/10.5194/egusphere-2024-641
Preprint. Discussion started: 14 March 2024

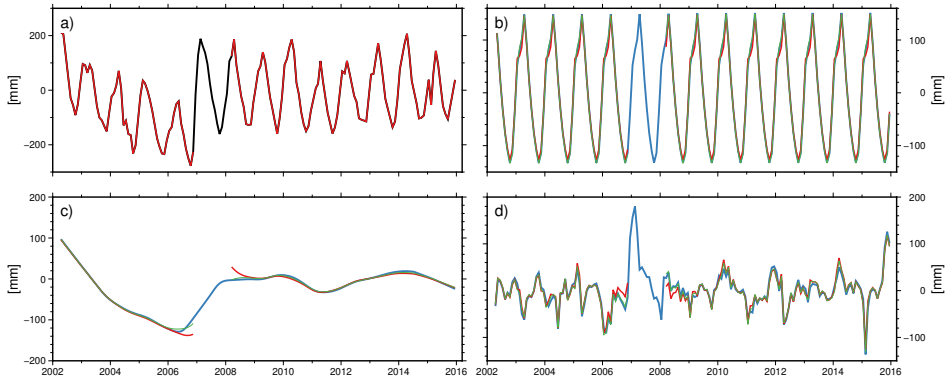

Figure 4. STL decomposition results of TWS time series (GRACE-only) at grid point 31.5°E, 5.5°S without data gap, with synthetically added data gap, and with filled data gap.

a) original TWS time series (black) and with data gap in 2007 (red); b) annual seasonal signal; c) interannual trend signal; d) residual. Blue lines: without data gap; red lines: standard STL gap filling; green lines: adjusted gap filling including seasonality.

about the clusters are needed. Hierarchical approaches produce a tree of clusters, where subsets at higher levels are created by merging two clusters from the next lower level. As the basis for computing the tree of clusters, we used the interannual trend component from the STL analysis. Pairwise Euclidean distances were determined to measure the similarity of the interannual TWS variations between the grid cells. We also considered the connectivity graph, which represents the k-nearest neighbours, to avoid a disjunct distribution of cluster members across the continent.

We decided on the final number of clusters based on their size. For more than 8 clusters, the smallest cluster only reached an overall size of roughly 700 km diameter, which is not meaningful in view of the spatial resolution of GRACE/GRACE-FO. Thus, as a result of the cluster analysis, eight regions of similar interannual TWS dynamics could be distinguished (Figure 5). The dendrogram of the clustering in Figure 6 gives an indication of the similarities between the different cluster regions. The length of the U-shaped legs in the dendrogram indicates the distance between clusters, i. e. longer legs equals larger distance. Cluster 2 encompasses most of the Sahara desert and has the largest distance to all other regions due to its lack of significant TWS signals. The island of Madagascar was fully assigned to cluster 7. Cluster 6 covers most of the Niger River basin and is the second African region with a strong positive trend. Large parts of the tropical rain forest (climate A according to Köppen-Geiger classification) are in cluster 3. The western part of southern subtropical Africa is clustered into cluster 5, which was wetting until around 2012 and subsequently drying again. Regions 1 and 4 encompass large parts of Africa and summarise regions with and without trends. The cluster of the East African Rift region (Label 0) shows a distinct temporal dynamic compared to the other African regions with strong non-linear interannual variability, i.e., a TWS decline until 2006 and an overall increase afterwards, culminating in a steep TWS rise in 2019 and 2020 and a subsequent decline. Among the regions with an overall positive TWS trend, the Rift cluster is the first that was separated out (Figure 6). Furthermore, it consists of two sub-clusters with a rather large distance. Figure 7 displays both the location of the two sub-clusters and their mean as well as cell-based interannual trend components. Sub-cluster 8 covers Lake Victoria and its direct surroundings and has even

https://doi.org/10.5194/egusphere-2024-641
Preprint. Discussion started: 14 March 2024

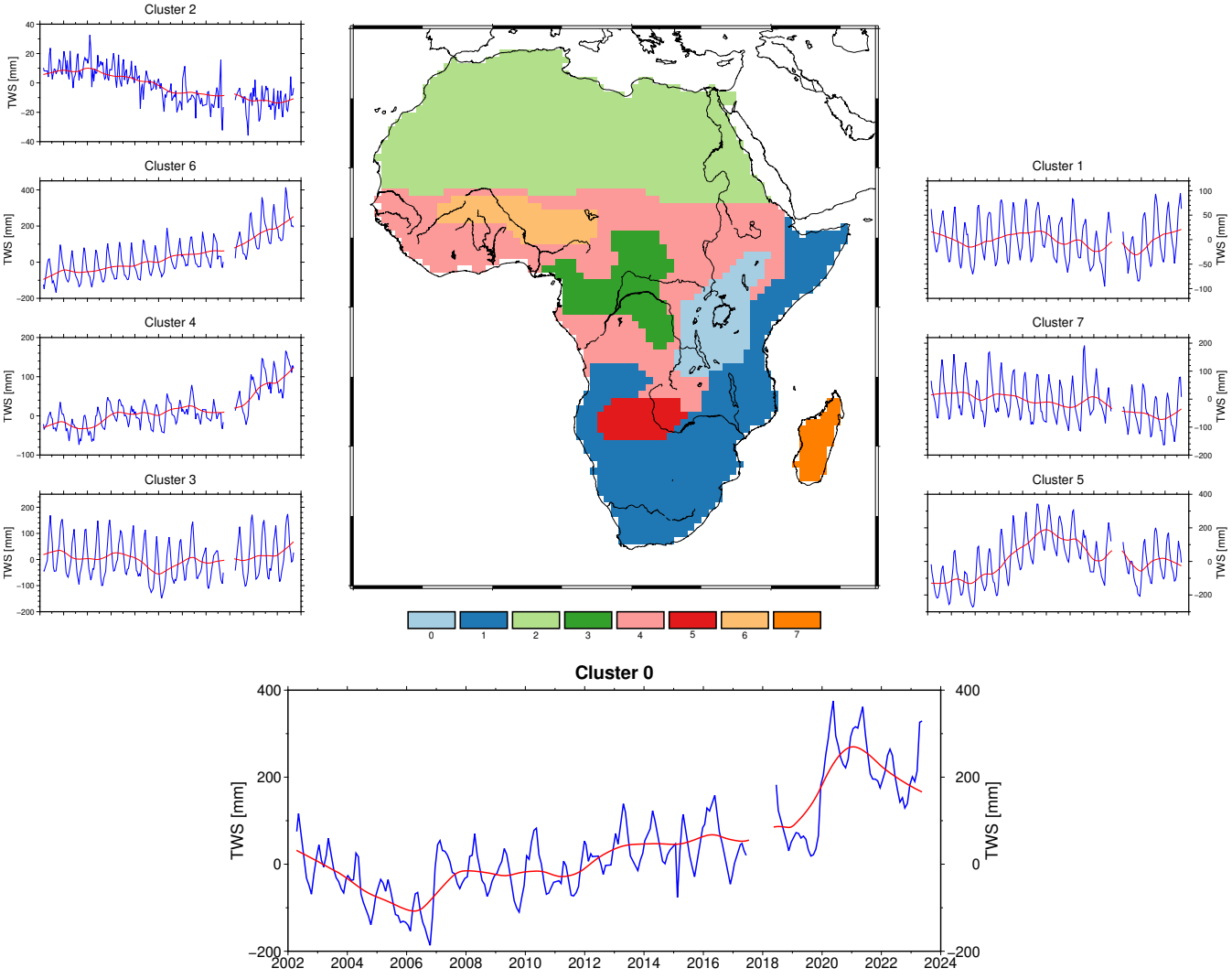

Figure 5. Cluster results for interannual TWS variability over Africa (centre). The mean TWS time series (blue) and the interannual trend component (red) from the STL analysis are shown for all clusters. Cluster 0 is the region of interest in the East African Rift.

https://doi.org/10.5194/egusphere-2024-641
Preprint. Discussion started: 14 March 2024

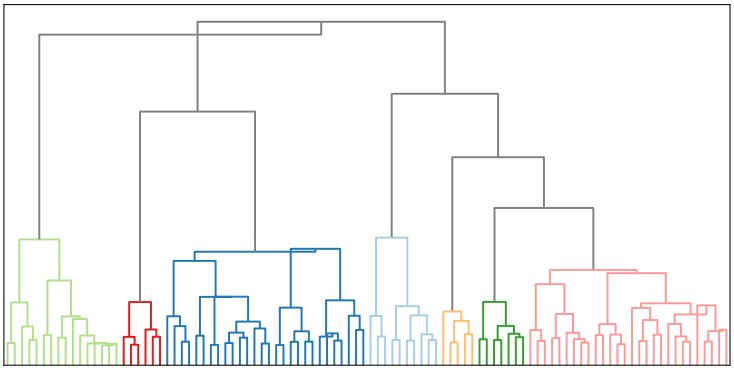

Figure 6. Dendrogram of the clustering (simplified). The colouring corresponds to the cluster map in Figure 5. (Madagascar cluster not included)

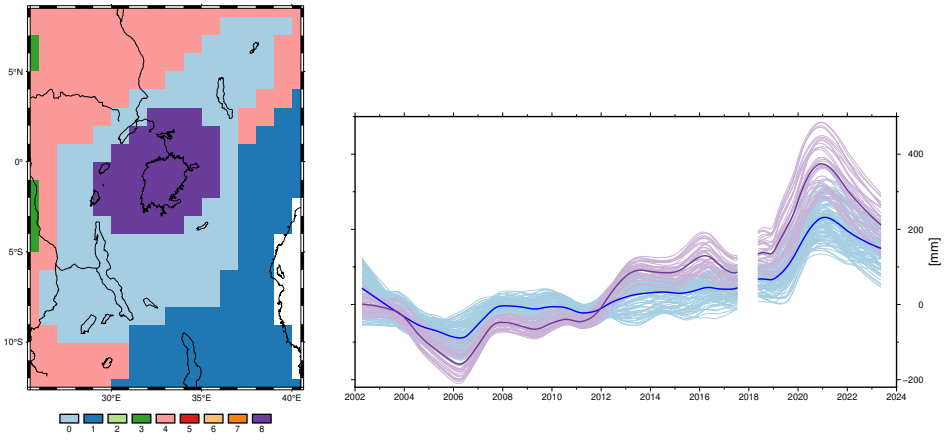

Figure 7. The two subclusters of the East African Rift region. The time series on the right hand side are coloured according to colours in the map (left hand side; blue sub-cluster 0, purple sub-cluster 8). Pale colours show all interannual time series of the subclusters; dark colours the mean time series.

larger TWS amplitudes than the other sub-cluster. Besides this, the most notable difference between the two sub-clusters is the marked TWS increase of sub-cluster 8 in 2012/13.

5 Comparison between TWS Signals and Precipitation

First, we compare the interannual TWS variations with precipitation. Monthly precipitation exhibits substantial short-term variability, not directly seen in the TWS observations due to their temporally integrating character. Thus, we compare accumu-

https://doi.org/10.5194/egusphere-2024-641
Preprint. Discussion started: 14 March 2024

lated precipitation with TWS. As we only investigate the interannual variability of TWS, the accumulation period should be an integer multiple of twelve months to remove the seasonality in precipitation. To this end, we investigate the correlation between TWS and accumulated precipitation with accumulation periods between 12 months (1 year) and 120 months (10 years). In Figure 8, the grid-wise correlation between the TWS and accumulated precipitation time series are plotted as violin plots. The median of all grid-wise correlations (green plus) and the correlations between the regional mean time series (red dot) are also marked. The median correlation and the correlations of the regional time series increase for accumulation periods until 36 or 48 months and then stay rather constant. However, the number of grid points with small or even negative correlations increases beyond the 48-month accumulation period. The constantly high correlation for accumulation periods longer then 48 months seems unexpected at first. However, the correlations are governed by the similarity of the two time series at the extreme points, the dryness around 2006 and the wetness around 2020. These two extreme are similarly well observed by accumulated precipitation beyond 48 months as long as the accumulation period stays below the 14 years time difference between the two events. Longer accumulation periods further smooths the time series which makes it similar to the smooth interannual TWS time series. We assume that we can transfer the investigation of the precipitation accumulation period to the following indices' investigations. We decided to use an accumulation period of 48 months rather then 36 months, as SPEI also shows an higher correlation to TWS with an accumulation period of 48 then 36 months (detailed results not shown here).

Considering only precipitation and its influence on TWS lacks an essential hydro-meteorological component in this tropical region: evaporation. We assume that precipitation minus (potential) evaporation predicts interannual TWS changes better than precipitation alone. For better comparability between precipitation minus evaporation and TWS, we use for the former not absolute values but standardised indices, the SPEI. That also allows us to put the precipitation minus evaporation in relation to long-term observations.

To this end, we employ two SPEI variants as introduced above (subsection 2.2). These indices indicate a surplus or lack of precipitation minus evaporation compared to a long-term mean (here since 1955).

Figure 9 presents the time series of the indices, TWS, and the accumulated precipitation. We used an accumulation period of 48 months for both indices and precipitation, as explained above. The relative shortage of precipitation from 2003 until 2006 caused the decline of TWS in these years. In these early years before 2008, the decline in TWS and subsequent rise fit also well with both indices. However, after 2008, TWS continuously rose while the precipitation stayed nearly constantly. Thus, increased precipitation cannot explain the storage increase between 2008 and 2016 alone. The high accumulated precipitation most probably caused the TWS increase in 2020-2022. SPEI (CRU-based) do show an increase in the years 2008-2016 but does not display a sharp increase around 2020. On the other hand, SPEI (GPCC-based) do not show an intermediate increase but a distinct increase in 2020. The differences between the two SPEI realisations can be caused either by substantial differences in the precipitation data sets after 2008, when the two indices started to diverge, or by the different PET estimations. The latter would affect the whole time series of SPEI, not only starting in 2008, which hints towards major differences in the precipitation. Both precipitation data sets are based on sparse interpolated station data over Africa which might explain the differences.

Overall, both SPEI indices strongly correlate with TWS with a correlation coefficient of 0.87 (CRU-based) and 0.82 (GPCC-based). The correlation between TWS and precipitation is 0.87 as well. As explained above, the correlation coefficients are

https://doi.org/10.5194/egusphere-2024-641
Preprint. Discussion started: 14 March 2024

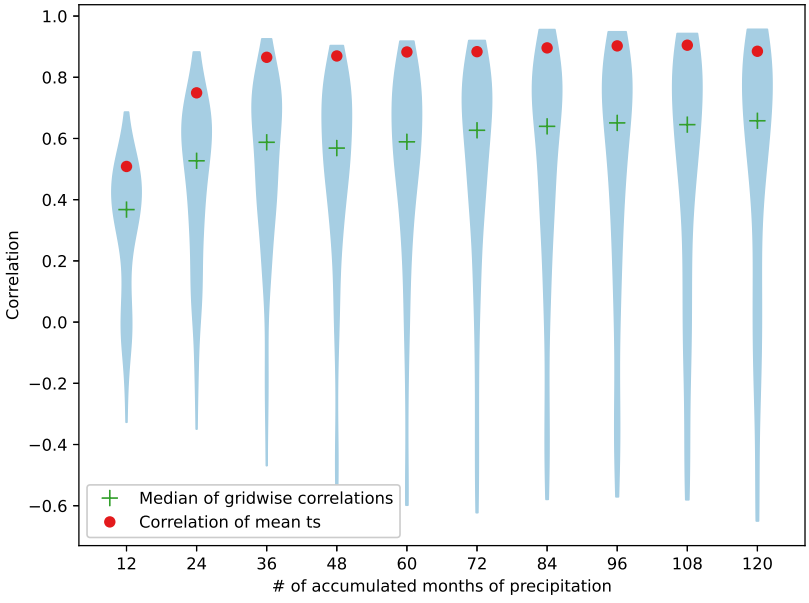

Figure 8. Correlations between precipitation with different accumulation periods and interannual TWS signal. The violin plot represents the scatter of the correlations in all grids. Green plus marks the median of these grid-wise correlations. Red dots indicates the correlation only between the regional mean time series.

govern by the two extreme points of the time series in 2006 and 2020. Which explains, that despise SPEI (CRU-based) being better able to describe the changes between the two extremes, precipitation has a similarly high correlation to TWS.

6 Comparison between TWS Signals and Surface Water Storage

The large lakes of the East African Rift (see Figure 2 for the names and locations) are a crucial component of terrestrial water storage in this region. We investigate the volume change of these lakes, i.e., surface water storage (SWS) variations, in comparison to TWS variations as observed by GRACE and GRACE-FO.

Overall, the linear trend of SWS over the study period from 2002 to 2023 can explain close to 50% of the TWS trend (Figure 10). However, the positive TWS trends in the North-East and South-West of the study area are less visible in the SWS trends. The lake storage trend of Lake Victoria itself (SWS-Victoria) is the most prominent component of SWS changes in the region, besides another marked contribution by Lake Tanganyika in the South-West. Notably, the filtered SWS-Victoria signal coincides with subcluster 8 shown in Figure 7. The storage time series at one grid point in the centre of the region at Lake Victoria (Figure 10)show a close temporal correlation of the three quantities TWS, SWS and SWS-Victoria. While TWS

https://doi.org/10.5194/egusphere-2024-641
Preprint. Discussion started: 14 March 2024

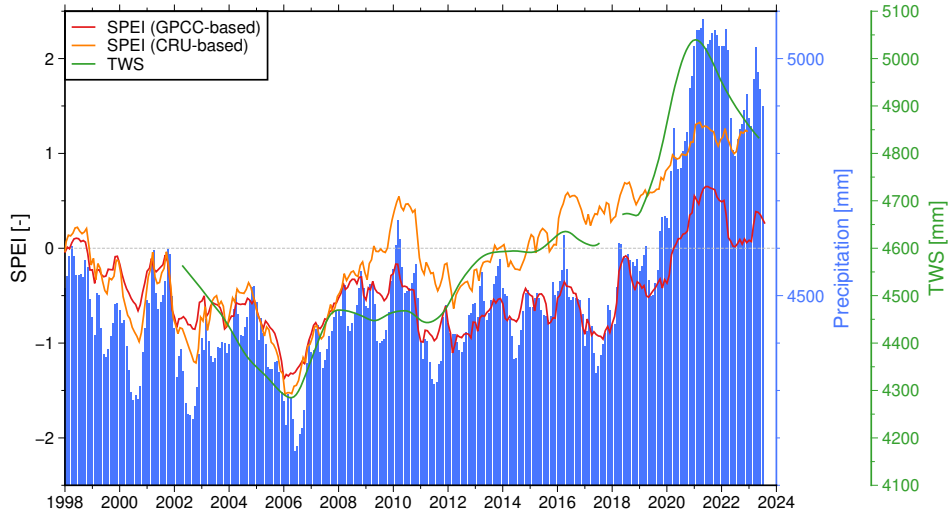

Figure 9. Comparison between SPEI (GPCC-based), SPEI (CRU-based), accumulated precipitation (accumulation period of 48 months), and TWS . Please note the different y-axes.

and SWS-Victoria are very similar in their dynamics, TWS has a higher amplitude and stronger annual fluctuations as it also represents other storage compartments, in particular soil moisture and groundwater.

For a closer look into the similarities of SWS and TWS dynamics, we show the percentage of explained variance (PEV) and Pearson's correlation coefficient (ρ) in Figure 11. PEV is defined as

$$PEV = \left(1 - \frac{var(TWS - SWS)}{var(TWS)}\right) 100\%. \tag{3}$$

PEV helps to evaluate to which extent the amplitudes of temporal variations of SWS can explain the variations of TWS. In the centre of the region around Lake Victoria, about 60% of the TWS variations can be explained by SWS. On the other hand, ρ describes the temporal similarities between the respective time series in each grid point and is insensitive to amplitude differences. We observe high temporal correlations between TWS and SWS throughout the study region, with the highest values around Lake Victoria, where the correlation is close to 1. From the corresponding analysis with SWS-Victoria (Figure 11, lower plots) it turns out that the storage variations of Lake Tanganyika in the South-West have to be considered to explain TWS variations. The wide-spread high temporal correlation between TWS and SWS (or SWS-Victoria) indicate that similar hydro-meteorological dynamics govern the whole region and its water storage.

To further investigate the storage contributions of the different lakes, we analyze the annual storage change of each year (i.e., the difference of storage between the end and the beginning of each year) for the individual lakes and for the area-average TWS. We only consider the volume change of the lake storage time series if less than two months are missing at the beginning or end of the year. In order to account for the missing months, the volume change is upscaled in these years. This is the case for Lake Albert in 2013, Lake Kivu in 2010 and 2013, Lake Mweru Matipa in 2010 and 2016, and Lake Edward in 2010 and 2013. For TWS, we only take years where observations both in January and in December are available.

https://doi.org/10.5194/egusphere-2024-641
Preprint. Discussion started: 14 March 2024

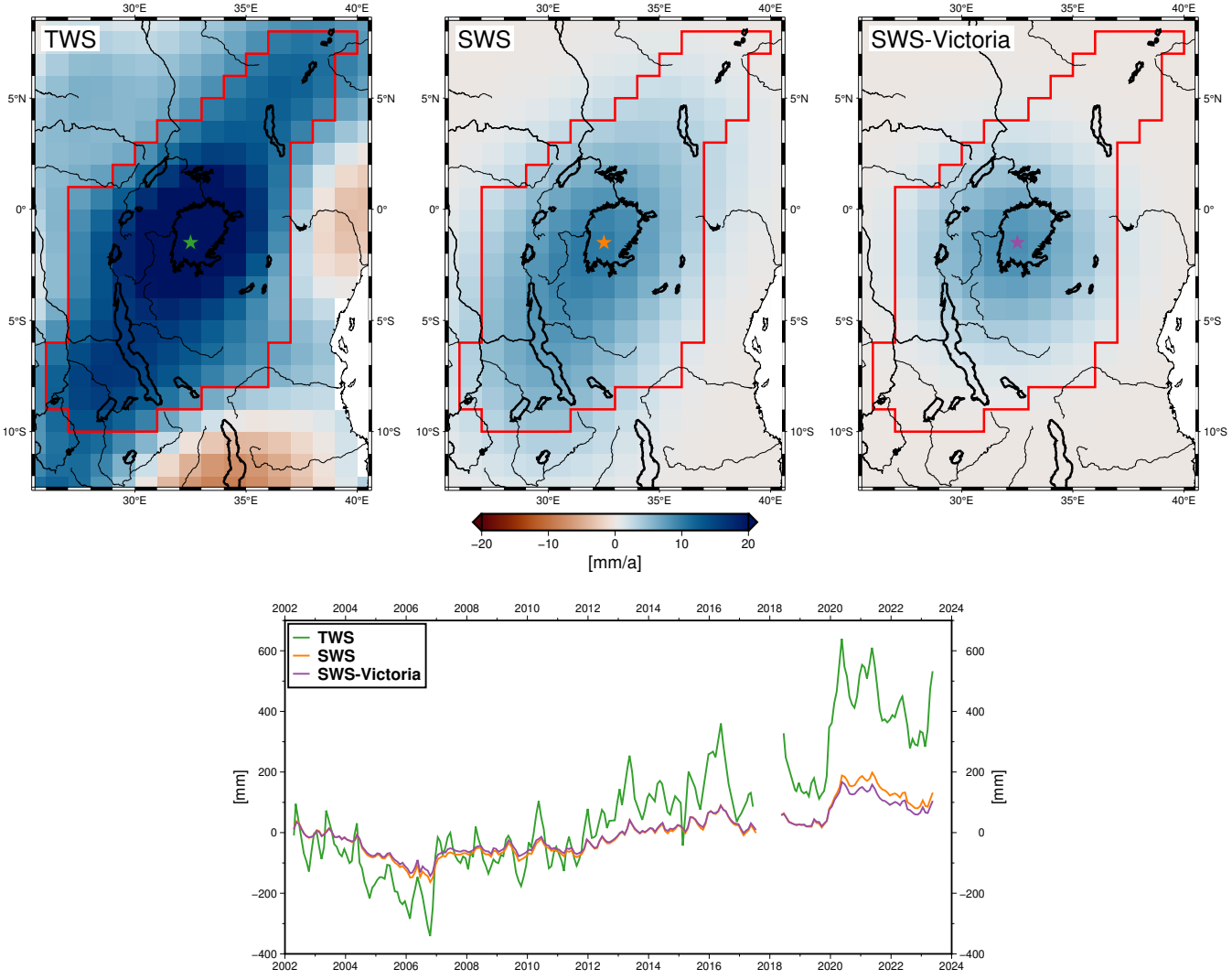

Figure 10. Upper plots: Linear trends for the period 2002-2023 of TWS, SWS (of all lakes), and SWS-Victoria (Lake Victoria only). The asterisk indicates the location of the de-seasonalized time series (1.5S, 32.5E) shown in the bottom panel.

https://doi.org/10.5194/egusphere-2024-641
Preprint. Discussion started: 14 March 2024

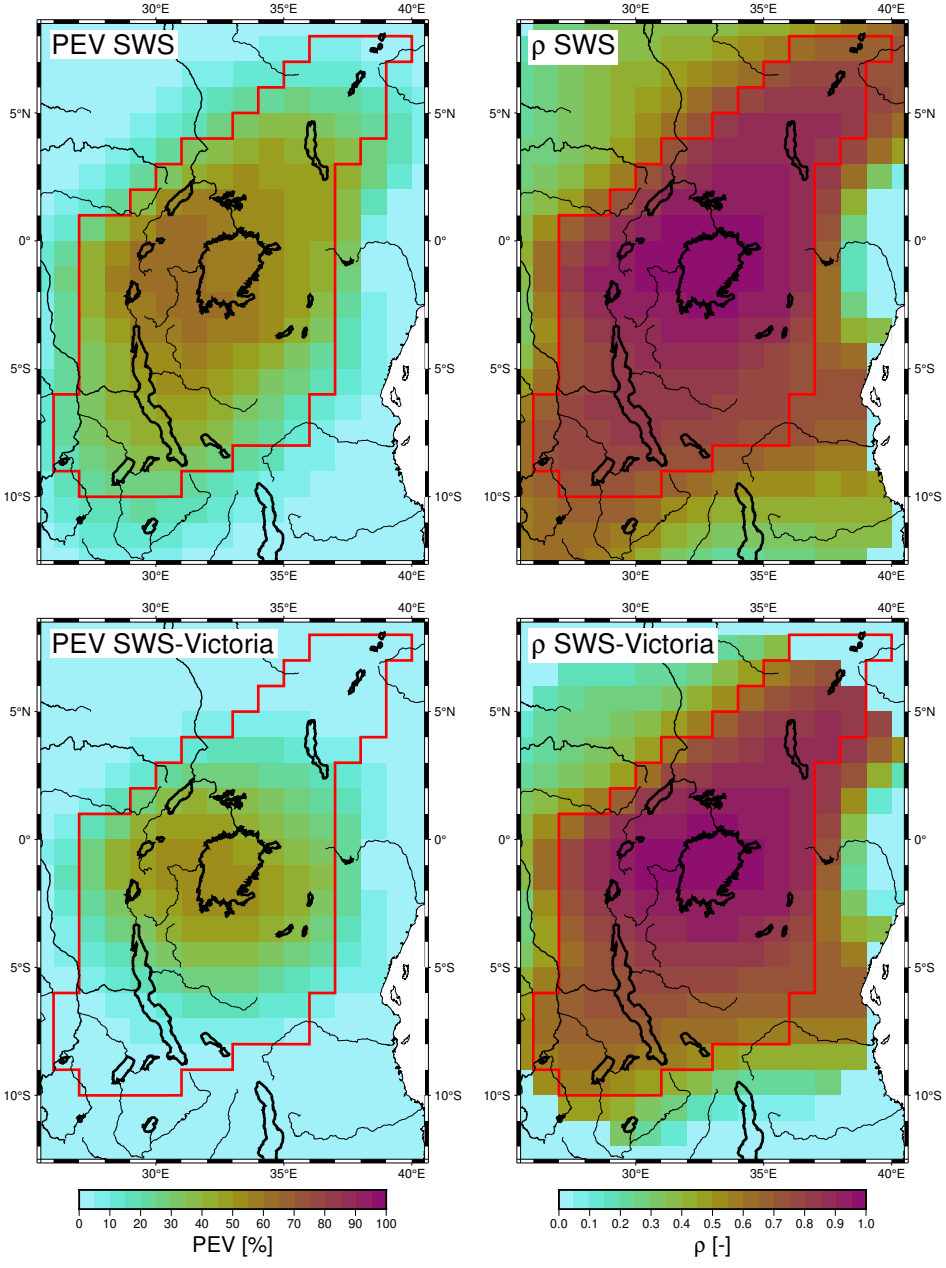

Figure 11. Left column: Percentage of explained variance PEV between filtered and de-seasonlaized SWS/SWS-Victoria and TWS; Right column: Pearson's correlation coefficient ρ between filtered and de-seasonlaized SWS/SWS-Victoria and TWS.

https://doi.org/10.5194/egusphere-2024-641
Preprint. Discussion started: 14 March 2024

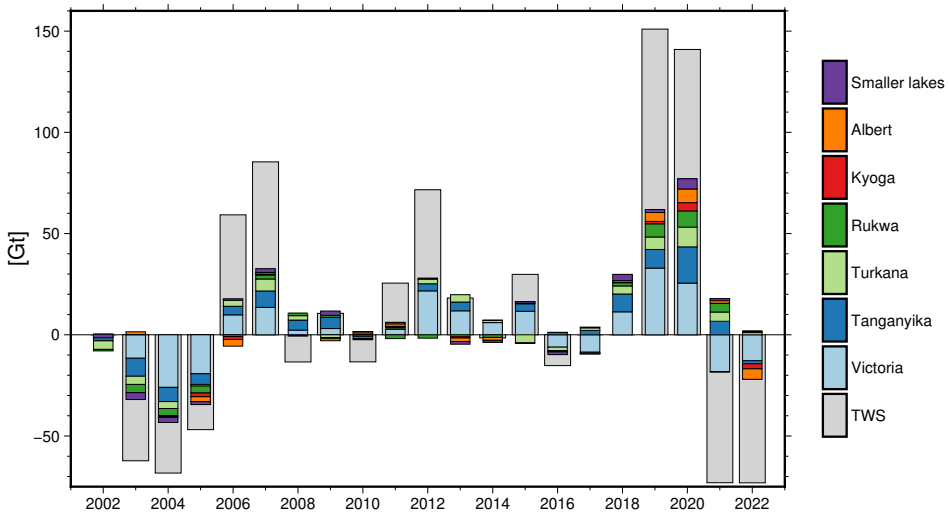

Figure 12. Annual TWS change of the Rift region (cluster 0) and change of water storage in lakes.

Figure 12 compares the annual TWS and lake volume changes. The volume changes of the lakes Mweru, Mweru Matipa, Kivu, and Edward (see Figure 2 green labelled lakes) are too small to be distinguishable from each other in the figure. Thus, we summarise these lakes as small lakes. In years with a substantial TWS change, the lake volumes usually agree with the direction of change. Especially, Lake Victoria exhibits the same direction of change as TWS, except in 2008 and 2014 which were years with overall minor changes. In some years such as 2013, Lake Victoria alone can explain over 50% of the TWS change of the whole region. Notably, Lake Albert and Lake Kyoga often disagree in the change direction with TWS. These lakes and Lake Victoria are located in the Nile River basin, which we will further investigate in the next section.

7 Dynamics of Lake Victoria and of downstream water bodies in the Nile Basin

In this chapter, we investigate the relation between the dynamics of Lake Victoria and of the Victoria Nile, Lake Kyoga and Lake Albert, located downstream of Lake Victoria in the Nile basin. As the Nalubaale Dam (formerly known as Owen Falls Dam) in Uganda regulates outflow and water levels of Lake Victoria it cannot be classified as a natural lake. The dam has been operated since 1954, and the reservoir on top of Lake Victoria was filled in the 1960s. This enlarged the lake volume by about 200 km^3 and raised the water level by about 2 m. It was agreed between the operators of the dam and the downstream riparians of the Nile that the outflow should mimic a natural discharge curve (after the water level rose in the 1960s) (Sene, 2000; Vanderkelen et al., 2018).

While we do not have access to the Victoria Nile discharge data downstream of the Nalubaale Dam, we use altimetric water level observations of Lake Victoria, the Victoria Nile and of the lakes Kyoga and Albert (Figure 13). Compared to the lake water levels, the quality of the Victoria Nile time series is poorer due to the comparatively small size and the challenging topography of the river for satellite altimetry. Sutcliffe and Parks (1999, chapt. 4) showed with historic discharge observations

https://doi.org/10.5194/egusphere-2024-641
Preprint. Discussion started: 14 March 2024

that the outflow of Lake Victoria almost completely determines the inflow and water level of Lake Kyoga. Thus, Lake Kyoga can be viewed as a proxy for direct observations at the Victoria Nile. We include Lake Albert to illustrate the natural flow between Lake Kyoga and Lake Albert. Again, according to Sutcliffe and Parks (1999, chapt. 4), the outflow of Lake Kyoga almost completely determines the water level of Lake Albert.

The different dynamics of Lake Victoria versus Victoria Nile and Lake Kyoga are particularly visible between 2006 and 2020 (Figure 13). While the former experienced a rather steady rise in water levels during the period, the water levels of the latter remained stable. This does not concur with the agreed rating curve as with rising water levels of Lake Victoria the discharge should increase and, thus, the water level of the Victoria Nile. The water levels of Lakes Kyoga and Albert show high similarities between each other but also to the temporal pattern of the Victoria Nile.

The change in the relation between the water levels over time is further illustrated in Figure 14. For this purpose, we interpolate the time series to common time steps, which are the time steps of the time series with a courser temporal resolution. Under natural conditions, the water levels of the three water bodies considered in this comparison should have a close, albeit not necessarily linear relationship, as explained above. We thus employ Spearman's rank correlation coefficient ρ_s to quantify the similarity of the water level time series. Only a weak relationship between the water level dynamics was found, with ρ_s in the range of 0.37 to 0.41 (Figure 14). The poor data quality of the Victoria Nile time series can partly explain the weaker Spearman's correlation between Lake Victoria and Victoria Nile as compared to the Lake Kyoga correlation. In contrast, with ρ_s equal to 0.88, water levels dynamics of Lake Kyoga are much more similar to those of the next downstream Lake Albert as it could be expected for neighbouring lakes.

Strictly speaking, we should consider the travel time of water between the lakes in the correlation analysis above. However, with Lake Kyoga only observed with Jason-series altimetry satellite, the temporal resolution is limited to 10 days. Thus, only a time shift of the time series larger than 10 days would be observable. The Victoria Nile between Lake Victoria and Lake Kyoga is about 120 km long (estimated on a map along the river path) and has an elevation difference of 100 m (measured by altimetry). We roughly estimate the flow velocity with the Gaukler-Manning-Strickler equation (Strickler, 1981) to 4.5 $\frac{m}{s}$ (assumption of constant river depth of 10 m, river width of 500 m, and literature value for large rivers for the Strickler coefficient of 35 $\frac{m^{\frac{1}{3}}}{s}$). Therefore, the travel time is only about 7.5 h, which is too fast for altimetry to observe a time shift.

If the outflow of Lake Victoria would be mainly govern by its water level, hardly any temporal variation of the relationship between the water levels of Lake Victoria on the one hand and Lake Kyoga and Victoria Nile on the other hand. However, according to Figure 14, the relationships between the water levels changed: before 2006, more water was released at the dam as expected from the water levels, as shown in previous studies. The dam operators discharged a surplus of water to help inaugurate a new 1 km downstream hydroelectric power plant named Kiira Power Station (Sutcliffe and Petersen, 2007; Kull, 2006; Awange et al., 2008). In the years between 2006 and 2019, the water level of Lake Victoria was rising while both the water levels of Lake Kyoga and the Victoria Nile stayed more or less constant, indicating that less water was released from the dam than the water level of the lake indicated. In 2020, the water levels of Lake Victoria quickly rose in a natural way due to the high amounts of rainfall on the lake and in its catchment, leading to severe flooding around the lake. By massively increasing lake outflow, these inundations were somewhat mitigated. These observations agree with the modelled results of

https://doi.org/10.5194/egusphere-2024-641
Preprint. Discussion started: 14 March 2024

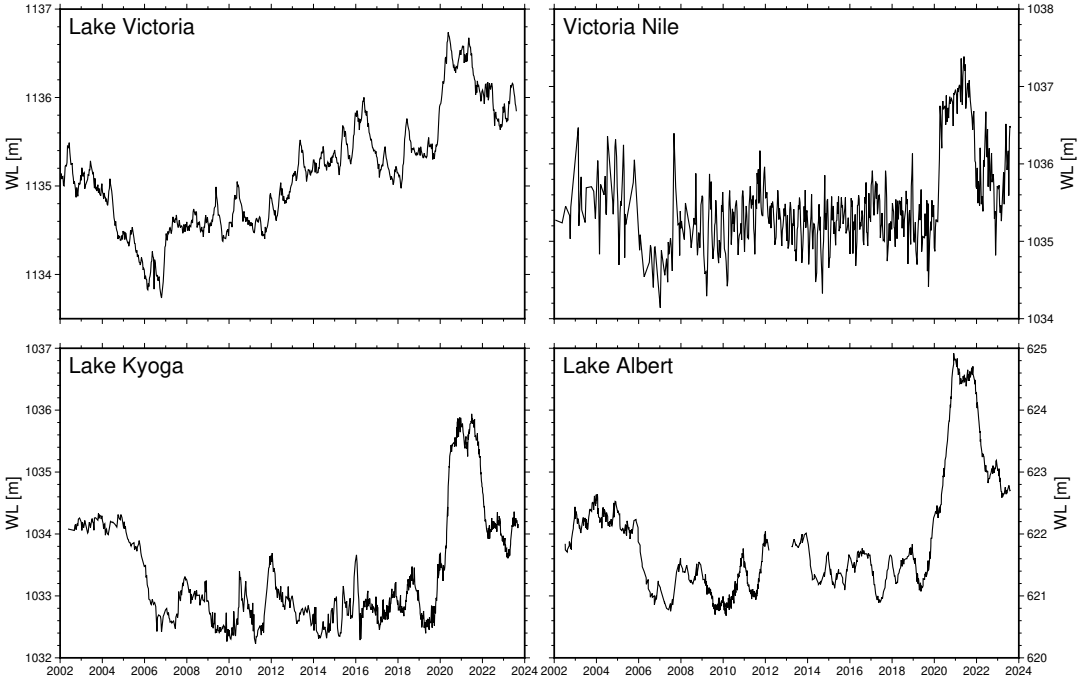

Figure 13. Water level of Lakes Victoria, Victoria Nile, Lake Kyoga and Lake Albert.

Vanderkelen et al. (2018); Getirana et al. (2020) who found that the storage variations of Lake Victoria cannot be explained by natural variations alone.

Instead of employing water level to assess the lake's discharge, we could also investigate volume changes (see section 6). However, the volume change is not only influenced by the inflow and outflow of a lake but also by evaporation over the lake's surface. Thus, again, it is only a proxy for the flow estimation. Investigations into volumes instead of water levels revealed no new information, so we refrained from presenting them here. Further, we could only investigate the lakes, not the Victoria Nile, with volume change.

8 Conclusions

Unlike other world regions with clear linear trends over the last 22 years of TWS observations (e. g. Northern India or the Caspian Sea), the East African Rift region, as well as most of Africa, shows a complex interannual behaviour. Further, the origin of these interannual variation can be both anthropogenic or due to natural variability.

A linear trend plus annual and semiannual seasonal signals describe the temporal patterns insufficiently only. To better investigate the interannual variability of TWS in Africa, we separated the TWS signal into an annual and an interannual component with the help of the Seasonal-Trend Decomposition with Loess (STL) method. Based on the interannual STL component we analysed the spatial patterns of similar interannual behaviour. To this end, these interannual signals were used

https://doi.org/10.5194/egusphere-2024-641
Preprint. Discussion started: 14 March 2024

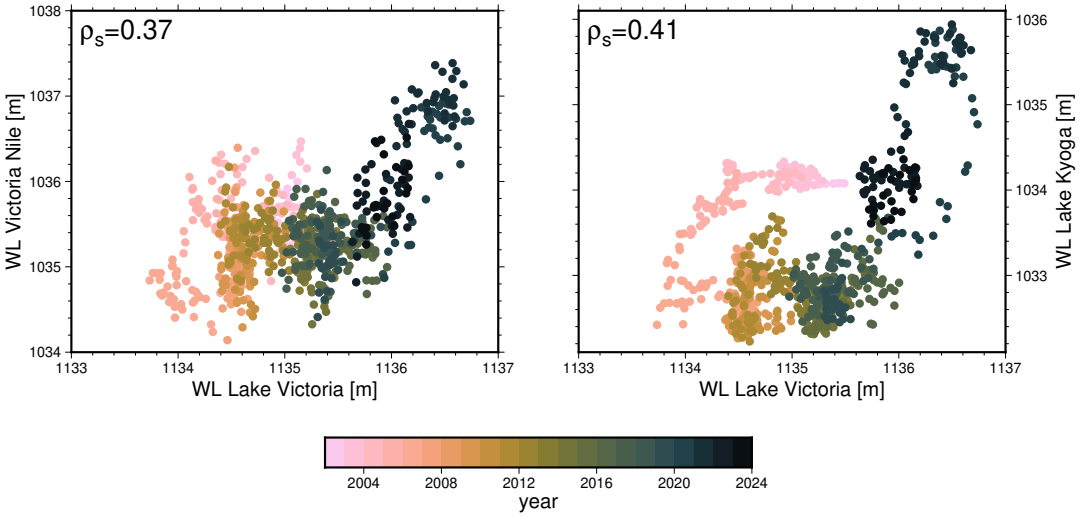

Figure 14. Relationships between the water levels of Lake Victoria and Victoria Nile (left plot) and Lake Victoria and Lake Kyoga (right plot).

in a geographical clustering algorithm to identify similar regions. The clustering algorithm is based on hierarchic trees but with the extension of ensuring geographically connected regions. With this method, the East African Rift region turned out to be of similar interannual TWS dynamics. The region encompasses the East African highlands, from Lake Turkana in the North to Lake Tanganyika in the South, including Lake Victoria.

The mean TWS signal of the study region shows a decline in water storage prior to 2006, linked to a documented natural drought period. Afterwards, TWS steadily increased until 2019. An even stronger TWS increase occurred in the years 2019 and 2020 due to severe rainfall events. Considering long-term precipitation data since 1955, these rainfall anomalies are less extreme than they seem when only looking into the last 20 years, though. By considering evapotranspiration in addition to rainfall, we could explain a larger part of the observed TWS changes as caused by natural variability. As another important storage component, surface water storage variations in the large lakes of the Rift region complemented the view on the interannual TWS signal. Water storage variations in Lake Victoria contribute up to 50% of the TWS variations. While it was not possible to explain the steady increase in TWS between 2006 and 2016 with meteorological data alone, this became possible with the help of lake storage variations.

Lake Victoria leads us back to whether the TWS changes we observe in the region are naturally caused or influenced by human interventions. The water level of Lake Victoria, and thus its water storage, is governed by the Nalubaale Dam at the lake outflow. Investigations into altimetric water levels of Lake Victoria, the Victoria Nile, Lake Kyoga, and Lake Albert indicate that the discharge at the dam does not follow a natural outflow pattern any longer and thereby influences TWS changes of the whole region. Thus, the combination of natural variability of precipitation and evaporation with human interventions cause the TWS interannual variations of the African Rift region.

https://doi.org/10.5194/egusphere-2024-641
Preprint. Discussion started: 14 March 2024

Code and data availability. The TWS data of COST-G used in this study have been published by Boergens et al. (2020a) and are available at ftp://isdcftp.gfz-potsdam.de/grace/GravIS/COST-G/Level-3/TWS. The data are published under the "CC BY 4.0" licence.

The water occurence map is available at https://global-surface-water.appspot.com and documented by Pekel et al. (2016). It is produced under the Copernicus Programme and is provided free of charge, without restriction of use.

The surface water storage time series, including water levels, water surface extent, volume change, and filtered map will be made available upon publication or earlier request.

The both SPEI data sets have been documented by Vicente Serrano, S.M., Beguiria, S. & Lopez-Moreno (2010); Beguería et al. (2010, 2014). SPEIbase can be downloaded at https://spei.csic.es/spei_database/; SPEI Global drought monitor can be downloaded at https://spei.csic.es/map/maps.html. Both are published under the ODbL 1.0 license.

The Python Code used for the clustering will be published upon manuscript publication.

Author contributions. EB and AG designed the study concept and discussion of the results with contributions of HD. EB did the implementation and lead of manuscript writing, including figure compilation. MS provided the clustering algorithm, and CS the altimetric water level time series. All authors contributed to the manuscript writing.

Competing interests. The authors declare that no competing interests are present.

Acknowledgements. We would like to thank Ulrich Meyer, University of Bern, for the computation of the COST-G gravity field product and Christoph Dahle, GFZ German Research Centre for Geosciences, for his contribution in the TWS processing. Qianheng Chen and Peter Morstein contributed to the development of the clustering algorithm.

https://doi.org/10.5194/egusphere-2024-641
Preprint. Discussion started: 14 March 2024

References

Anyah, R., Forootan, E., Awange, J., and Khaki, M.: Understanding Linkages between Global Climate Indices and Terrestrial Water Storage Changes over Africa Using GRACE Products, Science of The Total Environment, 635, https://doi.org/10.1016/j.scitotenv.2018.04.159, 2018.

Awange, J. L., Sharifi, M. A., Ogonda, G., Wickert, J., Grafarend, E. W., and Omulo, M. A.: The Falling Lake Victoria Water Level: GRACE, TRIMM and CHAMP Satellite Analysis of the Lake Basin, Water Resources Management, 22, 775–796, https://doi.org/10.1007/s11269-007-9191-y, 2008.

Ayugi, B., Tan, G., Niu, R., Dong, Z., Ojara, M., Mumo, L., Babaousmail, H., and Ongoma, V.: Evaluation of Meteorological Drought and Flood Scenarios over Kenya, East Africa, Atmosphere, 11, 307, https://doi.org/10.3390/atmos11030307, 2020.

Becker, M., LLovel, W., Cazenave, A., Güntner, A., and Crétaux, J.-F.: Recent Hydrological Behavior of the East African Great Lakes Region Inferred from GRACE, Satellite Altimetry and Rainfall Observations, Comptes Rendus Geoscience, 342, 223–233, https://doi.org/10.1016/j.crte.2009.12.010, 2010.

Beguería, S., Vicente Serrano, S. M., and Angulo-Martínez, M.: A Multiscalar Global Drought Dataset: The SPEIbase: A New Gridded Product for the Analysis of Drought Variability and Impacts, https://doi.org/10.1175/2010BAMS2988.1, 2010.

Beguería, S., Vicente Serrano, S. M., Reig-Gracia, F., and Latorre Garcés, B.: Standardized Precipitation Evapotranspiration Index (SPEI) Revisited: Parameter Fitting, Evapotranspiration Models, Tools, Datasets and Drought Monitoring, https://doi.org/10.1002/joc.3887, 2014.

Boergens, E., Dobslaw, H., and Dill, R.: COST-G GravIS RL01 Continental Water Storage Anomalies, https://doi.org/10.5880/COST-G.GRAVIS_01_L3_TWS, 2020a.

Boergens, E., Güntner, A., Dobslaw, H., and Dahle, C.: Quantifying the Central European Droughts in 2018 and 2019 with GRACE-Follow-On, Geophysical Research Letters, https://doi.org/10.1029/2020GL087285, 2020b.

Cleveland, R. B., Cleveland, W. S., McRae, J. E., and Terpenning, I.: STL: A Seasonal-Trend Decomposition, J. Off. Stat, 6, 3–73, 1990.

Dobslaw, H. and Boergens, E.: GFZ/COST-G GravIS Level-3 Products (V. 0005) Terrestrial Water Storage Anomalies, 2023.

Fan, Y. and van den Dool, H.: A Global Monthly Land Surface Air Temperature Analysis for 1948–Present, Journal of Geophysical Research, 113, D01 103, https://doi.org/10.1029/2007JD008470, 2008.

Ferreira, V. G., Asiah, Z., Xu, J., Gong, Z., and Andam-Akorful, S. A.: Land Water-Storage Variability over West Africa: Inferences from Space-Borne Sensors, Water, 10, 380, https://doi.org/10.3390/w10040380, 2018.

Frappart, F.: Groundwater Storage Changes in the Major North African Transboundary Aquifer Systems during the GRACE Era (2003–2016), Water, 12, 2669, https://doi.org/10.3390/w12102669, 2020.

Frappart, F. and Ramillien, G.: Monitoring Groundwater Storage Changes Using the Gravity Recovery and Climate Experiment (GRACE) Satellite Mission: A Review, Remote Sensing, https://doi.org/10.3390/rs10060829, 2018.

Getirana, A., Jung, H. C., Van Den Hoek, J., and Ndehedehe, C. E.: Hydropower Dam Operation Strongly Controls Lake Victoria's Freshwater Storage Variability, Science of The Total Environment, 726, 138 343, https://doi.org/10.1016/j.scitotenv.2020.138343, 2020.

Hassan, A. A. and Jin, S.: Lake Level Change and Total Water Discharge in East Africa Rift Valley from Satellite-Based Observations, Global and Planetary Change, 117, 79–90, https://doi.org/10.1016/j.gloplacha.2014.03.005, 2014.

Hastie, T., Tibshirani, R., and Friedman, J. H.: The Elements of Statistical Learning: Data Mining, Inference, and Prediction, Springer, 2 edn., 2009.

https://doi.org/10.5194/egusphere-2024-641
Preprint. Discussion started: 14 March 2024

Herrnegger, M., Stecher, G., Schwatke, C., and Olang, L.: Hydroclimatic Analysis of Rising Water Levels in the Great Rift Valley Lakes of Kenya, Journal of Hydrology: Regional Studies, 36, 100 857, https://doi.org/10.1016/j.ejrh.2021.100857, 2021.

Jäggi, A., Meyer, U., Lasser, M., Jenny, B., Lopez, T., Flechtner, F., Dahle, C., Förste, C., Mayer-Gürr, T., Kvas, A., Lemoine, J.-M., Bourgogne, S., Weigelt, M., and Groh, A.: International Combination Service for Time-Variable Gravity Fields (COST-G): Start of Operational Phase and Future Perspectives, in: Beyond 100: The Next Century in Geodesy, edited by Freymueller, J. T. and Sánchez, L., vol. 152, pp. 57–65, Springer International Publishing, Cham, https://doi.org/10.1007/1345_2020_109, 2020.

Khaki, M. and Awange, J.: The 2019–2020 Rise in Lake Victoria Monitored from Space: Exploiting the State-of-the-Art GRACE-FO and the Newly Released ERA-5 Reanalysis Products, Sensors, 21, 4304, https://doi.org/10.3390/s21134304, 2021.

Kull, D.: Connections Between Recent Water Level Drops in Lake Victoria, Dam Operations and Drought., Report, The Author, 2006.

Landerer, F. W., Flechtner, F. M., Save, H., Webb, F. H., Bandikova, T., Bertiger, W. I., Bettadpur, S. V., Byun, S., Dahle, C., Dobslaw, H., Fahnestock, E., Harvey, N., Kang, Z., Kruizinga, G. L. H., Loomis, B. D., McCullough, C., Murböck, M., Nagel, P., Paik, M., Pie, N., Poole, S., Strekalov, D., Tamisiea, M. E., Wang, F., Watkins, M. M., Wen, H.-Y., Wiese, D. N., and Yuan, D.-N.: Extending the Global Mass Change Data Record: GRACE Follow-On Instrument and Science Data Performance, Geophysical Research Letters, https://doi.org/10.1029/2020GL088306, 2020.

Lehmann, F., Vishwakarma, B. D., and Bamber, J.: How Well Are We Able to Close the Water Budget at the Global Scale?, Hydrology and Earth System Sciences, 26, 35–54, https://doi.org/10.5194/hess-26-35-2022, 2022.

McKee, T. B. T., Doesken, N. J. N., Kleist, J., McKee, Doesken, N. J. N., Kleist, J., Mckee, T. B. T., Doesken, N. J. N., and Kleist, J.: The Relationship of Drought Frequency and Duration to Time Scales. Eighth Conference on Applied Climatology. American Meteorological Society, Boston., Eighth Conference on Applied Climatology, https://doi.org/citeulike-article-id:10490403, 1993.

Meyer, U., Lasser, M., Dahle, C., Förste, C., Behzadpour, S., Koch, I., and Jäggi, A.: Combined Monthly GRACE-FO Gravity Fields for a Global Gravity-Based Groundwater Product, Geophysical Journal International, p. ggad437, https://doi.org/10.1093/gji/ggad437, 2023.

Okungu, J. O., Okonga, J. R., Mngodo, R. J., Sangale, F. D., Senfuma, N., Mjengera, H., Sewagude, S., and Mwembembezi, L.: Lake Victoria Water Levels., Report, Ministry of Water and Irrigation, 2005.

Olson, D. M. and Dinerstein, E.: The Global 200: Priority Ecoregions for Global Conservation, Annals of the Missouri Botanical Garden, 89, 199–224, https://doi.org/10.2307/3298564, 2002.

Pekel, J.-F., Cottam, A., Gorelick, N., and Belward, A. S.: High-Resolution Mapping of Global Surface Water and Its Long-Term Changes, Nature, 540, 418–422, https://doi.org/10.1038/nature20584, 2016.

Reager, J. T. and Famiglietti, J. S.: Global Terrestrial Water Storage Capacity and Flood Potential Using GRACE, Geophysical Research Letters, https://doi.org/10.1029/2009GL040826, 2009.

Rodell, M., Famiglietti, J. S., Wiese, D. N., Reager, J. T., Beaudoing, H. K., Landerer, F. W., and Lo, M.-H.: Emerging Trends in Global Freshwater Availability, Nature, 557, 651–659, https://doi.org/10.1038/s41586-018-0123-1, 2018.

Salvatore, M., Pozzi, F., Ataman, E., Huddleston, B., and Bloise, M.: Mapping Global Urban and Rural Population Distributions, 2005.

Sasgen, I., Wouters, B., Gardner, A. S., King, M. D., Tedesco, M., Landerer, F. W., Dahle, C., Save, H., and Fettweis, X.: Return to Rapid Ice Loss in Greenland and Record Loss in 2019 Detected by the GRACE-FO Satellites, Communications Earth & Environment, 1, 1–8, https://doi.org/10.1038/s43247-020-0010-1, 2020.

Scanlon, B. R., Rateb, A., Anyamba, A., Kebede, S., MacDonald, A. M., Shamsudduha, M., Small, J., Sun, A., Taylor, R. G., and Xie, H.: Linkages between GRACE Water Storage, Hydrologic Extremes, and Climate Teleconnections in Major African Aquifers, Environmental Research Letters, 17, 014 046, https://doi.org/10.1088/1748-9326/ac3bfc, 2022.

https://doi.org/10.5194/egusphere-2024-641
Preprint. Discussion started: 14 March 2024

Schneider, U., Hänsel, S., Finger, P., Rustemeier, E., and Ziese, M.: GPCC Full Data Monthly Version 2022 at 1.0°: Monthly Land-Surface Precipitation from Rain-Gauges Built on GTS-based and Historic Data: Globally Gridded Monthly Totals, https://doi.org/10.5676/DWD_GPCC/FD_M_V2022_100, 2022.

Schwatke, C., Dettmering, D., Bosch, W., and Seitz, F.: DAHITI - an Innovative Approach for Estimating Water Level Time Series over Inland Waters Using Multi-Mission Satellite Altimetry, Hydrology and Earth System Sciences, 19, 4345–4364, 2015.

Schwatke, C., Scherer, D., and Dettmering, D.: Automated Extraction of Consistent Time-Variable Water Surfaces of Lakes and Reservoirs Based on Landsat and Sentinel-2, Remote Sensing, 11, 1010, https://doi.org/10.3390/rs11091010, 2019.

Sene, K. J.: Theoretical Estimates for the Influence of Lake Victoria on Flows in the Upper White Nile, Hydrological Sciences Journal, 45, 125–145, https://doi.org/10.1080/02626660009492310, 2000.

Strickler, A.: Contributions to the Question of a Velocity Formula and Roughness Data for Streams, Channels and Closed Pipelines, WM Keck Laboratory of Hydraulics and Water Resources, Division of Engineering and Applied Science, California Institute of Technology, Pasadena, 1981.

Sutcliffe, J. V. and Parks, Y. P.: The Hydrology of the Nile, International Association of Hydrological Sciences Wallingford, Wallingford, 5 edn., 1999.

Sutcliffe, J. V. and Petersen, G.: Lake Victoria: Derivation of a Corrected Natural Water Level Series / Lac Victoria: Dérivation d'une Série Naturelle Corrigée Des Niveaux d'eau, Hydrological Sciences Journal, 52, 1316–1321, https://doi.org/10.1623/hysj.52.6.1316, 2007.

Swenson, S. and Wahr, J.: Monitoring the Water Balance of Lake Victoria, East Africa, from Space, Journal of Hydrology, 370, 163–176, https://doi.org/10.1016/j.jhydrol.2009.03.008, 2009.

Tapley, B. D., Bettadpur, S., Watkins, M., and Reigber, C.: The Gravity Recovery and Climate Experiment: Mission Overview and Early Results: GRACE MISSION OVERVIEW AND EARLY RESULTS, Geophysical Research Letters, 31, n/a–n/a, https://doi.org/10.1029/2004GL019920, 2004.

Tapley, B. D., Watkins, M. M., Flechtner, F., Reigber, C., Bettadpur, S., Rodell, M., Sasgen, I., Famiglietti, J. S., Landerer, F. W., Chambers, D. P., Reager, J. T., Gardner, A. S., Save, H., Ivins, E. R., Swenson, S. C., Boening, C., Dahle, C., Wiese, D. N., Dobslaw, H., Tamisiea, M. E., and Velicogna, I.: Contributions of GRACE to Understanding Climate Change, Nature Climate Change, 9, 358–369, https://doi.org/10.1038/s41558-019-0456-2, 2019.

Tong, X., Pan, H., Xie, H., Xu, X., Li, F., Chen, L., Luo, X., Liu, S., Chen, P., and Jin, Y.: Estimating Water Volume Variations in Lake Victoria over the Past 22years Using Multi-Mission Altimetry and Remotely Sensed Images, Remote Sensing of Environment, 187, 400–413, https://doi.org/10.1016/j.rse.2016.10.012, 2016.

Ummenhofer, C. C., Kulüke, M., and Tierney, J. E.: Extremes in East African Hydroclimate and Links to Indo-Pacific Variability on Interannual to Decadal Timescales, Climate Dynamics, 50, 2971–2991, https://doi.org/10.1007/s00382-017-3786-7, 2018.

Uwimbabazi, J., Jing, Y., Iyakaremye, V., Ullah, I., and Ayugi, B.: Observed Changes in Meteorological Drought Events during 1981–2020 over Rwanda, East Africa, Sustainability, 14, 1519, https://doi.org/10.3390/su14031519, 2022.

Vanderkelen, I., van Lipzig, N. P. M., and Thiery, W.: Modelling the Water Balance of Lake Victoria (East Africa) – Part 1: Observational Analysis, Hydrology and Earth System Sciences, 22, 5509–5525, https://doi.org/10.5194/hess-22-5509-2018, 2018.

Velpuri, N. M., Senay, G. B., and Asante, K. O.: A Multi-Source Satellite Data Approach for Modelling Lake Turkana Water Level: Calibration and Validation Using Satellite Altimetry Data, Hydrology and Earth System Sciences, 16, 1–18, https://doi.org/10.5194/hess-16-1-2012, 2012.

https://doi.org/10.5194/egusphere-2024-641
Preprint. Discussion started: 14 March 2024

Vicente Serrano, S.M., Beguiria, S. & Lopez-Moreno, J.: A Multi-scalar Drought Index Sensitive to Global Warming: The Standardized Precipitation Evapotranspiration Index - SPEI, Journal of Climate, 2010.

Ward, J. H.: Hierarchical Grouping to Optimize an Objective Function, Journal of the American Statistical Association, 58, 236–244, https://doi.org/10.1080/01621459.1963.10500845, 1963.

Yang, W., Seager, R., Cane, M. A., and Lyon, B.: The Annual Cycle of East African Precipitation, Journal of Climate, 28, 2385–2404, https://doi.org/10.1175/JCLI-D-14-00484.1, 2015.

Ziese, M., Becker, A., Finger, P., Meyer-Christoffer, A., Rudolf, B., and Schneider, U.: GPCC First Guess Product at 1.0°: Near Real-Time First Guess Monthly Land-Surface Precipitation from Rain-Gauges Based on SYNOP Data: Gridded Monthly Totals, https://doi.org/10.5676/DWD_GPCC/FG_M_100, 2011.